International Journal on Interactive Design and Manufacturing (IJIDeM)
https://doi.org/10.1007/s12008-023-01263-2

ORIGINAL PAPER

Experimentation with the EDM parameter through a full factorial technique and optimization using regression analysis with carbon nanotubes

Yashesh Darji[1] · Dilipkumar Patel[2] · Dhaval Patel[3] · R. Ramesh[4] · Ankit D. Oza[5] · Kiran S. Bhole[6] · Sachin M. Shinde[7] · Manoj Kumar[8]

Received: 9 September 2022 / Accepted: 17 February 2023

Abstract

Using an unconventional method of machining, electric discharge machining is capable of processing extremely hard materials that are inaccessible to more traditional machining methods. Electric discharge machining is a metalworking technique that uses an electric erosion effect in conjunction with an electrosparking spark. A current discharge takes place in a narrow space between the work piece and the electrode, melting and vaporizing the unwanted material and separating it from the parent metal in the process. When it comes to enhancing material removal rates and decreasing tool wear, powder-mixed electrical discharge machining is one of the most recent techniques. The machining mechanism, the cost-effectiveness of powder, the powder concentration in the working fluid, and the safety and environmental impact of this new development are just a few of the many questions that remain unanswered. As a result, it sees very little use in the manufacturing sector. EN-31 with aluminium as a tool electrode was examined in this study to determine its machining characteristics during EDM processing. The EDM procedure is used to study the MRR, TWR, and SR of the MWCNT combined with dielectric fluids. EDM process output parameters were predicted using regression models. Predictive models were built using the peak current, pulse on time, and pulse off time parameters of machining. In order to collect data, we used a full factorial design. ANOVA is used to identify the most influential input parameter that has the greatest impact on the final outcome. Using design expert software, the characteristics of EN-31 steel were improved and regression equations with and without MWCNT were compared using an electro-destructive method (EDM). Carbon nano tube combined as dielectric fluid improved surface roughness by an average of 30% while improving MRR by an average of 19% while decreasing TWR by 8.51 percent.

Keywords Powder mix EDM · TWR · MRR · Surface roughness · Multi wall carbon nanotubes (MWCNT) · Parameter optimization

✉ Ankit D. Oza
ankit.oza@iar.ac.in

Yashesh Darji
er.yash.dy88@gmail.com

Dilipkumar Patel
dspatel.mech@spcevng.ac.in

Dhaval Patel
dhaval05@gmail.com

R. Ramesh
mrramesh2002@gmail.com

Kiran S. Bhole
kiran_bhole@spce.ac.in

Sachin M. Shinde
sachin.shinde@dmce.ac.in

Manoj Kumar
manojkumar@abes.ac.in

[1] Department of Mechanical Engineering, Rai School of Engineering, Rai University, Ahmedabad, Gujarat 382260, India

[2] Department of Mechanical Engineering, Sankalchand Patel University, Visnagar, Gujarat 384315, India

[3] Department of Mechanical Engineering, Government Engineering College Palanpur, Palanpur, Gujarat 385001, India

[4] Department of Mechanical Engineering, SreeVidyanikethan Engineering College (Autonomous), Tirupathi, Andhra pradesh 517102, India

Published online: 18 March 2023

1 Introduction

High-precision fabrication of complex forms and small holes is made possible by the universal acceptance and widespread use of electrical discharge machining (EDM). [1].This method is used in a variety of industries, including metal bond diamond wheel profile truing, micro nozzle fabrication, composite drilling, and the manufacture of moulds and dies made from hardened steels. [2]. These materials are notoriously difficult to machine due to the high rates of tool wear and expense. The mechanical properties of tool steels have been studied extensively over the years for EDM; a dielectric fluid is used to create a vacuum between the tool and the work piece. Discharge energy at the spark's tip causes the surface of the work piece to reach very high temperatures. When the specimen is heated to temperatures of up to 40,000 K, a component of the work piece melts and evaporates [2] In this process, the top surface of the work piece rapidly re-solidifies and cools. Heat-treated tool steels and high-tech materials (super alloys, ceramics, and metal matrix composites) are being machined with EDM technology in the tool, die, and mould industries due to its ability to achieve high precision, complex shapes, and high surface polish [3].The removal of material and the rate of tool wear are important considerations in traditional machining. Nanotubes of carbon. (CNTs) [4]

Genomic expression programming (GEP) to predict roughness levels based on experimental data and indicated that the GEP model and SR can be linked via a mathematical relationship [5] EDM has also been employed on the same material with electrodes made of copper, copper–tungsten (W–Cu), and graphite, all with Taguchi method-designed experimental settings [6]. EDM machining properties were examined in relation to magnetic force.

In addition, a Taguchi-based L18 orthogonal array was used in this study to carry out a series of experiments, and the experimental data were statistically analysed using analysis of variance (ANOVA). The response surface methodology was suggested [7] for the modelling and study of the rapidly re-solidified SG cast iron layer in the EDM process. ANOVA results show that the suggested mathematical model may appropriately describe the performance within the constraints of the components being evaluated.

[5] Department of Computer Sciences and Engineering, Institute of Advanced Research, The University for Innovation, Gandhinagar, Gujarat 382426, India

[6] Department of Mechanical Engineering, Sardar Patel College of Engineering, Andheri West, Mumbai 400058, India

[7] Department of Mechanical Engineering, Datta Meghe College of Engineering, Airoli, Navi Mumbai 400078, India

[8] Department of Mechanical Engineering, ABES Engineering College, Ghaziabad, Uttar Pradesh 201009, India

Electrical discharge machining is an important machining centre in die manufacturing. EDM is a thermal process by which conductive material can be machined using electric discharges [2]. The process is based on applying a voltage between the tool electrode and the work piece while both are immersed in a dielectric fluid [8]. During the process, the tool and work piece are at a distance of microns when a plasma channel is created between the anode and cathode. Most of the electrical energy is transformed into thermal energy and the material melts or vaporizes instantly [9]. There is no contact between the tool and the work piece and the use of thermal energy for machining make this technology highly suitable for applications where really hard materials are used. Problems such as residual stress, chatter and other vibrations due its negligible cutting force is not there since there is no contact between electrode and the work piece [10]. The main constraint of the EDM machining is significant amount of tool wear. Furthermore process is only applicable for conductive material [11].

The most common materials that are used for EDM operations are copper, tungsten copper. These are basically used for high degree of good surface finish. If nano surface textures are to be created then use silver tungsten and RC type pulse generator is done which produces low amount of energy [12]. It's the best material for micro EDM since it material removal rate is high, low electrode wear. Further they also reveal about the EDM process as the thermo electrical process where the material eruption is done by the action of the sparks that are generate between the terminals of the machine. One terminal is the electrode, whose profile is intended on the work piece. Other is the work piece itself. The negative polarity of the electrode helps to achieve the highest material rate [13]. Now a day generally electrode is used as the positive terminal keeping into mind about the electrode wear. Both of the terminals are separated by the die electric medium [14]. There are many function of the die electric medium, which are as follows: acts as conductor, coolant, and the flushing medium for cleaning the carbon particles between the two terminals. Light petroleum based oil is used as the die electric medium [15]. The surface Ra ranges from 0.2 to 13 Micrometers. Refer Fig. 1 for the same. Some of the advantages which are obtained are.

a. Complex shapes which would not be possible by CNC milling can be obtained by EDM.
b. Extremely hard material to very close tolerances can be machined.
c. Very small work pieces where conventional cutting tools may damage the part from excess cutting tool pressure.
d. There is no direct contact between tool and work piece. Therefore delicate sections and weak materials can be machined without any distortion.
e. A good surface finish can be obtained.
f. Very fine holes can be drilled.

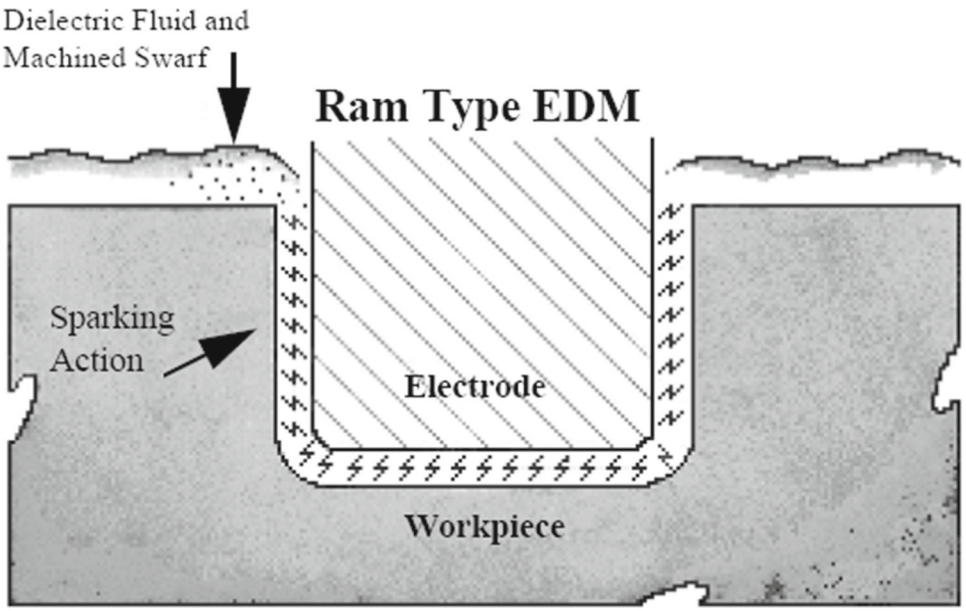

Fig. 1 Concept of EDM

Further they have explained about the *orbital moment* of the current is an important factor in EDM machining, the orbital feeding moment which is used in finishing operation in the EDM. The theory revels about cutting process which is observed during EDM [16] While roughing operation is in action current is made to flow through the electrode only in Z direction. Hence it can be concluded that the electrode wear is observed at the bottom face of the electrode. Some amount of stock about 0.05 is kept for finishing. When the finishing operation is stared the electrode which was entering the cavity earlier through the roughing cycle does not enter in the finishing cycle. In the finishing cycle the current pattern is made to swing in the XY plane hence the cutting is observed at the top most point. Sparks are observed at the top of the cavity [17].

After successive sparking cycles the electrode will reach the bottom of the cavity, spark mark can be observed on the electrode surface. When full current is allowed to flow through the electrode at that time only the cavity size that is to be generated. Full current means the current which is proportion to the spark gap. Usually for graphite 250 pattern for 0.25 mm spark gap. Generally for different shapes of electrodes, flow the pattern is decided. The pattern decides the no of vector that are included in the pattern [18]. More the number of vectors more, more would be the deflection of the current in the electrode periphery more will be the amount of current touching the exact profile and trying to finish the electrode profile [19]. Orbital moment is shown in Fig. 2

2 Carbon nano tube

CNTs and graphite are closely connected. Because of its hexagonal carbon atom rings, graphite's molecular structure resembles a planar network of stacked, one-atom-thick chicken wire. Carbon sheets are often piled one on top of the other in traditional graphite, making it easy for them to glide over one another. As a result, graphite is a lubricant rather than a hard material [4]. The edges of graphene sheets are joined to form a cylinder, which is how MWCNT is created. (Table 1). There are only tangents between the graphitic planes, hence their properties are more like those of a molecule, as stated in the section above [20]. High frequency vibrations in carbon–carbon bonds create an intrinsic thermal conductivity that is higher than diamond's. Figure 3 shows TEM pictures of multiwall carbon nanotubes obtained from Cheap tubes Inc. in the United States. Because of the unique features of carbon nanotubes (CNTs), researchers are particularly interested in nano-fluids containing CNT nano-fluids. CNTs can be thought of as having the basic structure of a cylinder or a collection of concentric cylinders [21]. When the effective thermal conductivity of MWCNTs was evaluated in synthetic (poly—olefin) oil, they achieved the highest thermal conductivity enhancement ever achieved in a liquid [22]. When liquid lubricants fail due to factors like extreme heat or pressure, solid lubricants might be an excellent alternative. Weak molecular bonds between the several layers are thought to be the cause of their lubricating capabilities. It is this ability to slide with minimal force that gives these layers their low-friction qualities. The aircraft sector uses CNT because of its excellent strength-to-weight ratio.

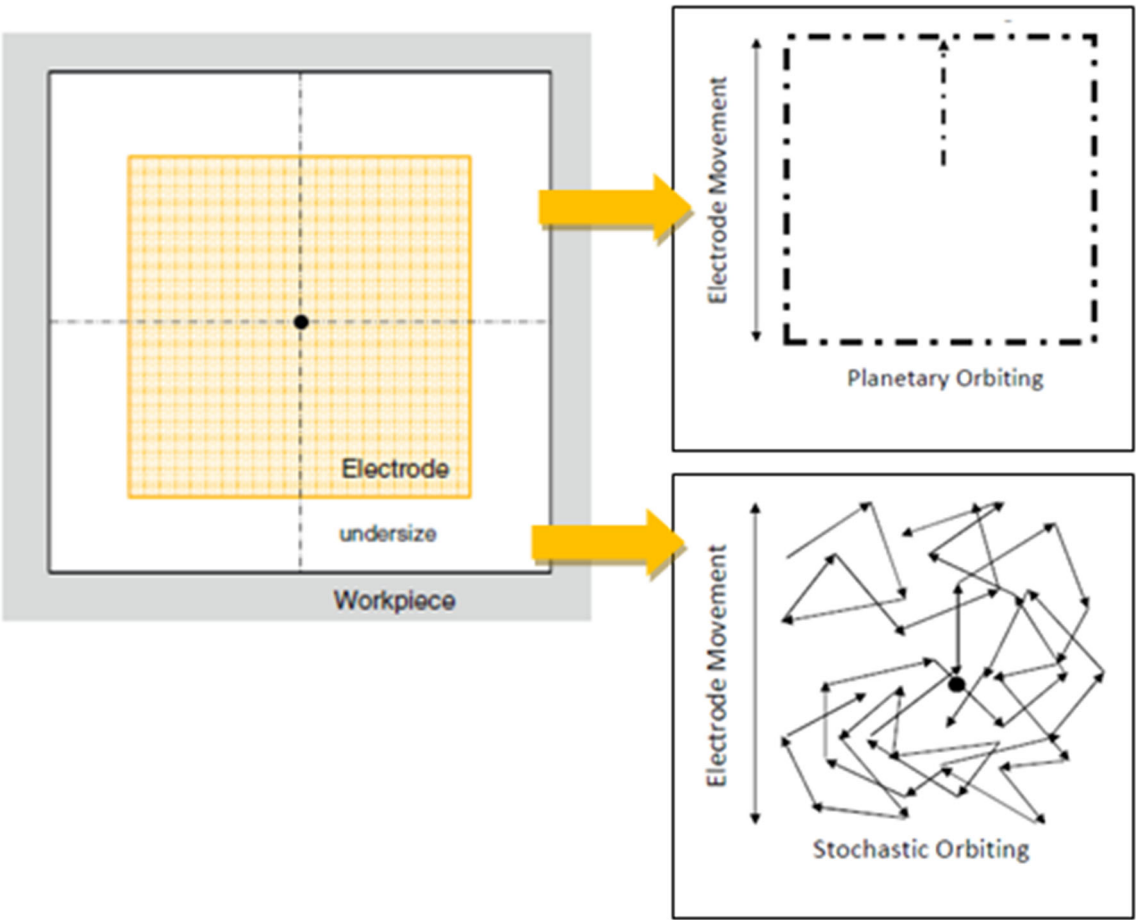

Fig. 2 Stochastic orbiting movement of the electrode in XY plane

Table 1 EN-31's primary characteristics

Material	Thermoelectric properties (W/mk)	Density (g/cc)	Resistance to electricity	Capacity to generate heat (J/g- 'c)
EN-31	46.6	7.81	0.0000218	47.5×10^{-3}

More than one trillion times more than the Young's modulus of C-fibre, CNT's Young's modulus is over one trillion times greater than the Young's modulus of aluminum at 70 GPa. A 500-fold increase in the strength-to-weight ratio compared to aluminium. One hundred percent greater than any other material's maximum strain Axial thermal conductivity of 3000 W/mK contrasts sharply with the low radial thermal conductivity of the material. Copper has a conductivity of 106 A/cm^2 and CNTs have a conductivity of 109 A/cm^2 [4]. A high aspect ratio CNT with an extremely high current carrying capacity and an efficient field emitter. In order to assess the surface quality of component parts, we use the Hommel Tester TR500 SR model as a multi-purpose measuring device. SR may be checked on a plane, cylinder, groove, and bearing raceway with this tool.

3 Experiments process a flow chart

Analyzing EDM parameters such as MRR, TWR and Surface Roughness using CNT mixed dielectric fluids is discussed in this study. CNT mixed dielectric machining has never been used before. Full Factorial data collection with coded levels for three machining parameters and an ANOVA and regression model were utilized to collect experimental data on the effects of CNT-based nano fluid on material removal rate, tool wear rate, and surface roughness. Design expert software and regression equations were utilized to optimize the properties of the En-31 tool steel using multiwall carbon nanotubes used in EDM process.

Pieces of EN-31 were formed utilizing a 15 mm diameter aluminium tool and a 30^3 mm geometrical cube cube of work piece material. Experiment was carried out using a Z 50

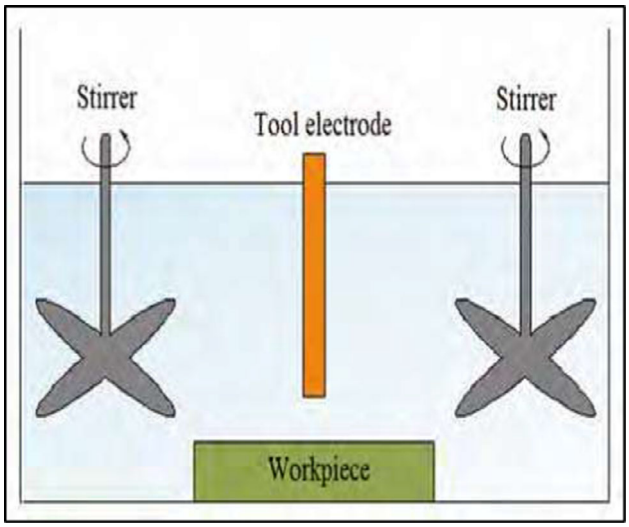

Fig. 3 Transmit the powder, use twin stirrers

Fig. 4 Prototype tank for EDM

JM-322 EDM machine. Both regular kerosene and MWCNT mixed kerosene are common dielectric fluids. Three EDM parameters, include parameters like pulse on/off duration and peak current, are manipulated in this experiment. In order to solve a three-part issue, 27 die sinking EDM tests are performed. The output parameters include material removal rate, surface roughness, and tool ratios. It is possible to compute the material removal rate using a 200-g weight machine with a 0.01-g precision, and the results are analyzed and optimized using DX 8 Statistical software and a regression for predication.

Using a larger container to mix the powder in the EDM machine is not recommended because of the machine's larger container. In order to prevent powder particles from mingling, we need to build the container in a way that prevents them from accumulating as shown in Figs. 3 and 4 Furthermore, when using the machine's existing circulation system, the filter may become clogged due to powder particles and debris. A new 6.0-L container for dielectric fluid was built at the workshop. In this container, investigations were carried out on the EDM machine that was already there. (Fig. 5) Two unique stirrers are fastened to the new prototype tank to ensure that the powdered dielectric fluid in the discharge gap between the tool electrode and the work piece material is properly circulated. The dielectric fluid was spiked with 0.5 g/l of CNT. Figure 6 shows the experimental setup.

4 Regression analysis

Independent variables and dependent variables can be analyzed using a regression model. Here, surface roughness serves as the dependent variable, and pulse current, pulse on duration, and pulse voltage serve as the independent variables. Die sinking EDM machining and its correlation to MRR TWR and SR Ra machining parameters like peak current, pulse on time, and pulse off time.

The connection between the input and output parameters can be evaluated with the help of empirical expressions. Empirical formulas for Surface roughness have been built using average output values. The peak current, pulse on time, and pulse off time of the EDM process were utilized to create an empirical model for MRR TWR & SR.

4.1 Regression analysis of MRR, TWR & SR without and with CNT

$Y = a_0 + a_1x_1 + a_2x_2 + a_3x_3$.
Y = MRR, TWR and SR.a = coefficient
X_1 = peak current.
X_2 = pulse on time.
X_3 = pulse off time. Where Y is the true value on the logarithmic scale of the output of the dependent machine, × 1, × 2, and × 3 are the logarithms of the respective input parameters, and a0, a1, a2, and a3 are the estimated values of the corresponding parameters. Regression analysis was performed to calculate the coefficients a1, a2, and a3; these values were then utilized to estimate the parameters of the aforementioned first order model in Microsoft Excel.

5 Calculation of MRR, TWR and surface roughness

5.1 Evaluation of MRR

The material MRR is expressed as the ratio of the difference of weight of the work piece before and after machining to

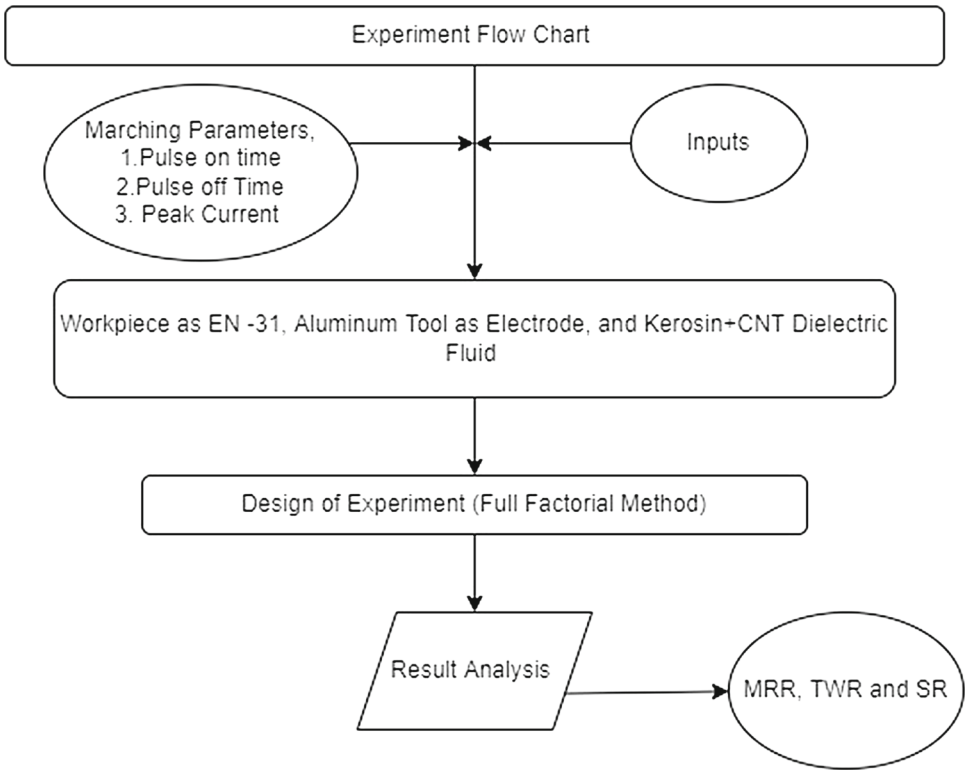

Fig. 5 Experiment Flow Chart

Fig. 6 Experimental Setup on Electric Discharge Machine

the machining time and density of the material.

$$MRR = \frac{Wjb - Wja}{t\delta}$$

where as Wjb = Weight of work piece before machining.

Wja = Weight of work piece after machining.t = Machining time, ℘ = Density of EN-31 steel material

Unit of MRR: mm^3/min.

5.2 Evaluation of tool wear rate

TWR is expressed as the ratio of the difference of weight of the tool before and after machining to the machining time. That can be explaining this equation.

$$TWR = \frac{Wtb - Wta}{t\delta}$$

whereas Wjb = Weight of the tool before machining.

Wta = Weight of the tool after machining.t = Machining time.

Unit of TWR: mm^3/min.

6 Conduct of experiments

The work piece material as EN-31 was particulate using Aluminum tool with 15 mm diameter and work piece dimension

Table 2 MWCNT specification

Aspect ratio	~1000
Specific surface area	350 m^2/g
Purity –wt%	> 95%
Metallic impurity	< 5%
Outer diameter	20–40 nm
Inner diameter	5 nm
Number of walls	5–15
Length	50 μm

were 30 × 30 × 30 mm square cube. JOEMARS—Made: Z 50 JM-322 EDM machine was used for conducting experiment. Commercial kerosene and also MWCNT mixed kerosene used as dielectric fluid. In this experiment three EDM parameters such as pulse on time, pulse off time and peak current are varied at three levels of each. For a three factor are tackled with a total number of 27 experiments performed on die sinking EDM. Three responses such as material removal rate and surface roughness and tool were ratios are measure as output parameters. The material removal rate and tool were ratio are calculated by using weight machine having the capacity of 200 g and accuracy is 0.01 g which is shown in Fig. 4.7 and surface roughness was measured by using Mitutoyo SJ 201P Surface roughness tester having display range between 0.01 μm and 100 μm. (Table 2)

Predicted MRR and experimental MRR are compared in Table 3. The margin of error (in percentage) is provided as well. The actual MRR and the anticipated MRR are graphed in Figs. 7 and 8 respectively. Results for the MRR with and without CNT are extremely similar, as can be observed. The values predicted by the empirical model are quite close to the observed ones.

A summary of the differences between the calculated TWR and the measured TWR is provided in Table 4. The margin of error (in percentage) is provided as well. The actual TWR and the anticipated TWR are plotted, respectively, in Figs. 9 and 10. Comparing the anticipated TWR with and without CNT, it is clear that the numbers are fairly close. The values predicted by the empirical model are quite close to the observed ones. Refer Table 5.

Predicted SR and experimental SR are compared in Table 6. The margin of error (in percentage) is provided as well. Graphs of observed and anticipated SR are presented in Figs. 11 and 12, respectively. Observed and anticipated SR values for both cases (with and without CNT) are quite close. The values predicted by the empirical model are quite close to the observed ones.

7 Results and discussion

7.1 Effect of peak current for without CNT MRR, TWR and SR

Between 17 and 28A, the peak current (I_p) is linearly proportional to MRR. As a result, the temperature rises, and more material is melted and eroded off the work piece as a result of the increased peak current. Although the other element has a little effect on I_p, comparable findings were made by [2] [24]. MRR, on the other hand, increases as the discharge current rises from 17 to 28 A. A rise in MRR was seen from 11.535 to 49.407 mm^3/min as the peak current was increased from 17 to 28 A.

As can be seen from the experiment results, TWR increases as Peak current rises. Peak Current in the 17–28 A range shows an increase in tool wear while the tool wear rate is decreasing. The melting and evaporation of the electrode rises as I_p, increases, resulting in greater heat energy being generated at the tool-work piece interface. It's reasonable to conclude that I_p has a direct impact on TWR.

Experimental results show that SR increases in correlation with increasing Peak current. The roughness of the surface is rising as the peak current rises from 17 to 28 A. More current means more energy in each discharge and a larger crater, thus as I_p grows, the pulse energy increases and consequently more heat energy is produced at the tool-work piece contact. In other words, it's reasonable to conclude that I_p has a large impact on SR.

7.2 Effect of pulse on time for without CNT MRR, TWR and SR

Results show that the rise in Pulse on time results in an increase in the MRR. An essential input parameter that has a considerable impact on the rate of material removal is pulse on time. Spark energy is induced over a longer period of time when the pulse on time is increased, resulting in larger craters on the work piece, which indicates a high MRR. The pulse durations in this experiment are 45, 55, and 65 microseconds.

The results of the experiment show that TWR increases as pulse on time increases. Pulse on time and I_p effects on TWR the TWR values are shown to be higher when the pulse on time is increased. Total machining time is used to calculate the tool wear ratio. In order for the electrical discharge machining process to work effectively and efficiently. Thermal energy dissipates more readily from a collision location when pulse on time is increased, as does discharge energy into electrodes as plasma channel size and electrode thermal conductivity rise in parallel. Because additional heat energy is spread from the spark struck position, the quantity

Table 3 Error for predicted MRR and experimental MRR (Without & with CNT)

Exp. no	Without CNT MRR			With CNT MRR		
	Exp	Regression	Error (%)	Exp	Regression	Error (%)
1	17.363	16.0258632	7.70107	20.5282	19.12052748	6.857262
2	49.407	43.79905675	11.3505	58.9771	52.60060221	10.81182
3	37.885	36.63039008	3.311627	45.0263	43.8097911	2.701774
4	19.867	18.11175209	8.834992	23.9258	21.36278303	10.71236
5	27.996	27.38719116	2.174628	34.0935	32.7996092	3.795125
6	19.127	20.65314098	− 7.97899	22.5067	24.63706081	− 9.46545
7	20.649	20.21852449	2.084728	24.4133	24.00879809	1.656892
8	13.503	12.44152987	7.860995	16.0645	14.72512192	8.337502
9	18.197	19.17558005	− 5.3777	21.6962	22.88767031	− 5.49161
10	21.968	22.75991338	− 3.60485	26.4802	27.28307587	− 3.03199
11	38.611	35.58744564	7.830811	46.8544	42.68866332	8.890812
12	32.261	30.96016786	4.032213	38.897	37.17212999	4.434455
13	11.535	8.857196535	23.21459	13.5397	10.32971637	23.70794
14	25.566	28.4301356	− 11.2029	30.1985	33.92073698	− 12.3259
15	33.414	34.54450119	− 3.38332	40.1502	41.56753554	− 3.53008
16	29.789	32.01446894	− 7.47077	35.3863	38.31614253	− 8.2796
17	15.974	13.48447431	15.58486	18.8221	15.8462497	15.81041
18	22.254	21.69608542	2.507031	26.2374	25.75818859	1.826444
19	16.044	15.59124671	2.821948	19.11	18.49226476	3.232523
20	23.292	25.28041876	− 8.53692	27.983	30.15359415	− 7.75683
21	17.853	17.06880765	4.392496	21.2325	20.24165526	4.666642
22	24.63	27.37583453	− 11.1483	29.1569	32.77672443	− 12.415
23	37.49	39.17177897	− 4.48594	45.0554	47.08406888	− 4.50261
24	43.038	40.21472342	6.559962	52.0845	48.20519665	7.448096
25	21.108	24.84580227	− 17.708	25.1016	29.52533142	− 17.6233
26	27.636	32.00311231	− 15.8023	32.9476	38.29325777	− 16.2247
27	21.675	23.80285783	− 9.81711	25.5418	28.40420364	− 11.2067

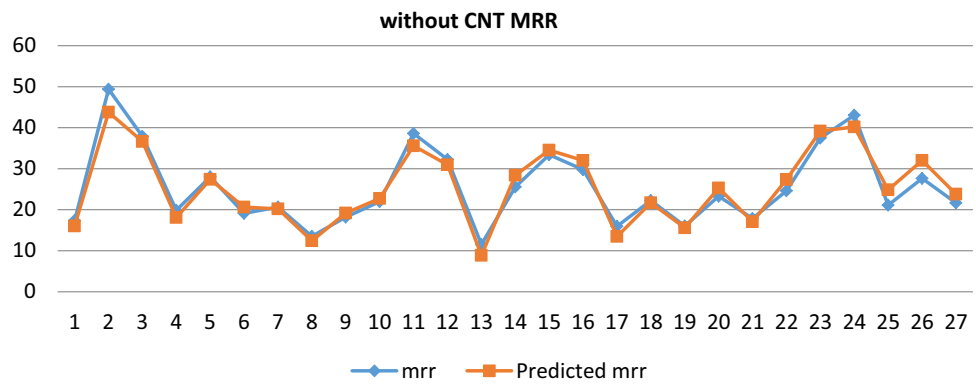

Fig. 7 Graph illustrating the discrepancy between observed and expected MRR in the absence of CNT

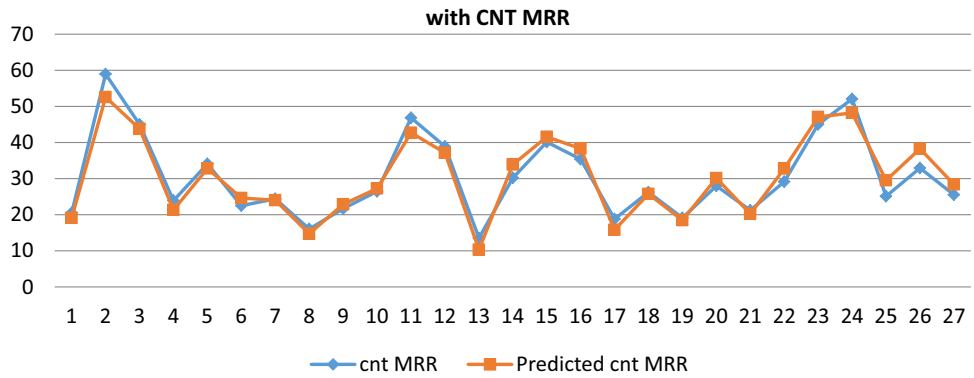

Fig. 8 Graph Illustration of the discrepancy between observed and expected MRR with CNT

Table 4 Variation between calculated and measured TWR (Without & with CNT)

Exp. no	Without CNT TWR			With CNT TWR		
	Exp	Regression	Error (%)	Exp	Regression	Error (%)
1	2.129	1.896778973	10.90752	1.967	1.755185783	10.76839
2	6.962	6.913080048	0.702671	6.451	6.371225209	1.236627
3	5.438	6.17330227	− 13.5216	5.03	5.684669654	− 13.0153
4	3.591	3.332778973	7.190783	3.294	3.059296894	7.12517
5	4.882	4.017585424	17.70616	4.507	3.705200119	17.7901
6	2.871	2.984667861	− 3.95917	2.647	2.750519116	− 3.91081
7	3.529	3.277807646	7.117947	3.271	3.018644564	7.714932
8	1.045	1.526890084	− 46.1139	0.956	1.411908005	− 47.6891
9	2.886	2.559807646	11.30258	2.654	2.366589008	10.82935
10	2.931	2.929696535	0.044472	2.723	2.709866786	0.482307
11	5.262	5.45530227	− 3.67355	4.867	5.032614098	− 3.4028
12	3.826	4.367413381	− 14.1509	3.531	4.037280765	− 14.3382
13	1.258	1.157001195	8.028522	1.165	1.068630227	8.272084
14	5.092	4.735585424	6.999501	4.661	4.357255675	6.51672
15	4.189	4.73730227	− 13.0891	3.907	4.380558542	− 12.1208
16	5.727	5.105474313	10.85255	5.264	4.700533453	10.70415
17	2.124	2.244890084	− 5.69162	1.953	2.06396356	− 5.6817
18	2.257	3.702667861	− 64.0526	2.11	3.402574671	− 61.2595
19	2.956	2.189918757	25.91614	2.724	2.023311231	25.72279
20	3.126	4.07255675	− 30.2801	2.855	3.745852449	− 31.2032
21	2.056	2.614778973	− 27.178	1.898	2.407241338	− 26.8304
22	3.257	3.997524492	− 22.7364	3.001	3.694002987	− 23.0924
23	6.148	5.825191159	5.250632	5.645	5.375891876	4.767194
24	6.985	6.543191159	6.325109	6.39	6.027947431	5.665924
25	4.881	4.365696535	10.55733	4.489	4.013977897	10.58191
26	5.273	5.085413381	3.557493	4.86	4.68933632	3.511598
27	4.779	3.647696535	23.67239	4.396	3.361922342	23.52315

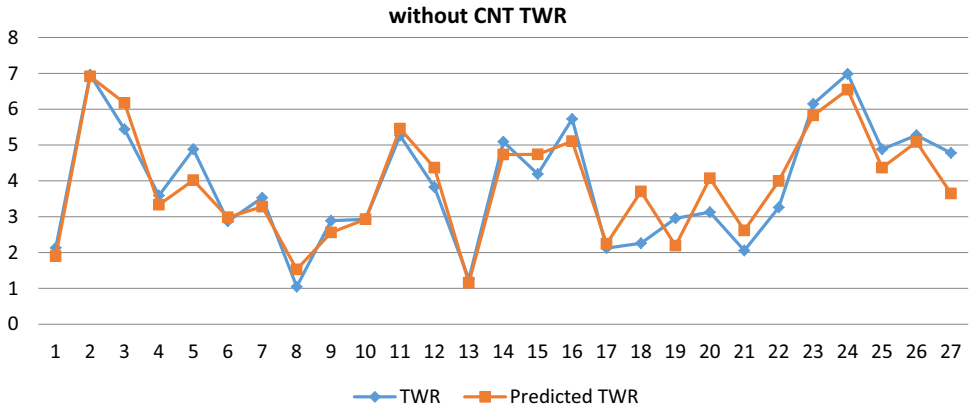

Fig. 9 Graph Comparison of measured and projected TWR for without CNT

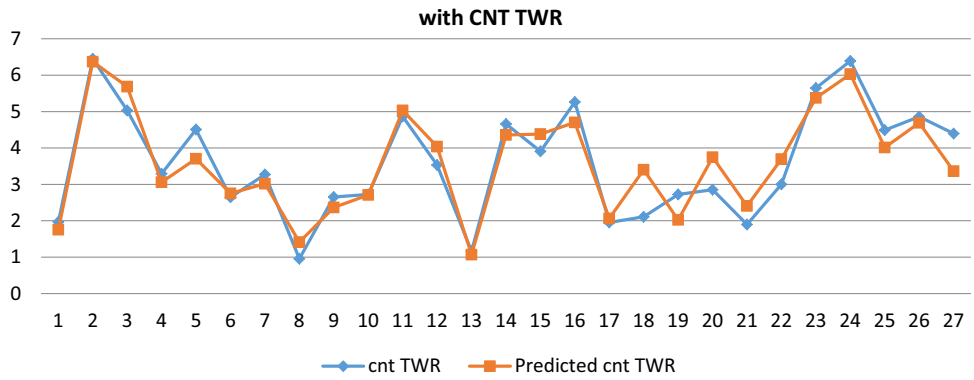

Fig. 10 Graph Comparison of measured and projected TWR for with CNT

of heat transmitted from the plasma channel to the electrodes increases, resulting in a drop in plasma channel efficiency as the molten crater on the electrodes grows in size.

The increase in SR can be seen as a result of an increase in pulse rate over time. For a given amount of pulse on time, there will be more spark energy generated into the workpiece, which will result in larger holes in the workpiece, an indication of high surface roughness. The pulse lengths used in this experiment are 45, 55, and 65 micro seconds. Surface roughness is a function of pulse on time. The increase in spark energy and the resulting widening of electrical discharge pores on the workpiece's surface occurs as the pulse on time grows, and this causes an increase in surface roughness.

7.3 Effect of pulse off time for without CNT MRR, TWR and SR

MRR decreases as pulse off time increases, according to the results. Pulse off time has a direct impact on non-machining time and MRR. The MRR was low at a small value of pulse off time, but it spiked dramatically as the pulse off time was increased. [page needed] Slowly, the MRR began to decline as pulse off time increased. Short pulse-off times have a significant chance of producing arcing because the gap dielectric may not have restored its original dielectric strength completely. In addition, the discharge gap may still include debris particles after it has been cleaned. The MRR would be low as a result. Debris particles are flushed out of the gap when the pulse-off time is long enough. As the pulse-off time is increased, the MRR decreases slowly because machining does not occur during this time and it only adds to the non-machining time. Increased pulse off duration reduces MRR since the additional benefit of dielectric strength recovery was not accessible. As can be seen from the data, TWR decreases as pulse off time increases. Increasing the pulse off time increases non-machining time while lowering TWR. During non-machining periods, EDM machines do not emit sparks, hence pulse off times are less influenced.

The graph shows that the SR decreases as the pulse off time increases. As the pulse off-time increases, so does the surface roughness, possibly as a result of the dielectric being adequately flushed and deionized over the longer pulse off-time.

Table 5 Difference between expected and experimental SR error (Without & with CNT)

Exp. No	Without CNT SR			With CNT SR		
	Exp	Regression	Error (%)	Exp	Regression	Error (%)
1	8.894	9.860088411	− 10.8622	6.478	7.285862605	− 12.4709
2	15.593	15.53464576	0.374234	11.443	11.4617945	− 0.16424
3	14.139	14.51353465	− 2.64895	10.177	10.7117945	− 5.25493
4	11.373	11.42464397	− 0.45409	8.169	8.348529271	− 2.19769
5	12.814	12.27615472	4.197325	9.51	9.051565114	4.820556
6	11.147	11.15292174	− 0.05312	8.141	8.192195938	− 0.62887
7	10.256	11.25504361	− 9.74106	7.473	8.301565114	− 11.0874
8	9.57	9.349532855	2.303732	6.922	6.910862605	0.160899
9	10.577	10.47276583	0.98548	7.828	7.77023178	0.737969
10	11.078	10.98332139	0.854654	8.223	8.14523178	0.94574
11	13.565	13.73125687	− 1.22563	9.951	10.18046117	− 2.30591
12	12.647	12.43842354	1.649217	9.424	9.274127838	1.590324
13	7.346	8.8389773	− 20.3237	5.545	6.535862605	− 17.8695
14	12.817	13.0584325	− 1.88369	9.636	9.582898447	0.551075
15	12.673	12.94897909	− 2.17769	9.734	9.649127838	0.871915
16	13.847	13.56898805	2.007741	10.092	9.957898447	1.328791
17	11.418	10.13181063	11.26458	8.477	7.442195938	12.2072
18	13.548	11.93519952	11.90434	9.81	8.723529271	11.07513
19	10.428	9.962210275	4.466722	7.721	7.39523178	4.219249
20	10.565	12.44575508	− 17.8018	7.82	9.098529271	− 16.3495
21	11.82	10.64236619	9.963061	8.639	7.817195938	9.512722
22	12.146	11.92786798	1.795917	9.05	8.899127838	1.667096
23	14.625	14.24181243	2.620086	10.596	10.55546117	0.382586
24	14.972	15.0240902	− 0.34792	11.232	11.0867945	1.292784
25	11.776	12.54787694	− 6.55466	8.86	9.207898447	− 3.92662
26	13.164	13.22070131	− 0.43073	9.815	9.805461171	0.097186
27	12.455	11.76559916	5.535133	9.302	8.676565114	6.72366

7.4 Effect of MWCNT-dielectric fluid on MRR

The maximum rate of reaction (MRR) with MWCNT and kerosene dielectric mixer at 28A and 65A microsecond pulse on time and 30 microsecond pulse off time was 58.097 mm^3/min, while that for pure kerosene was 49.407 mm^3/min. The findings of the experiments demonstrate that a 0.5 g/l concentration of MWCNT powder caused the EDM process to become unstable. Cai-Miao Hong and colleagues According to the graph, the MRR increases with an increase in Peak current and pulse on time. Kerosene may be to blame for this increase in MRR increasing concentration. Whencircuit break, additive particles are added to dielectric fluid, reducing its insulating strength. Particle striking and powder density could have their ideal relationship at this concentration, as well.

7.5 Effect of MWCNT-dielectric fluid on TWR

The MWCNT and kerosene Mixer had a mean TWR of 0.956 mm^3/min, whereas pure kerosene had a mean TWR of 1.045 mm^3/min at 17A and a pulse on time of 45 micro seconds. The CNT powder content was found to be 0.5 g/l. The graph shows that the peak current, pulse on time, and CNT concentration are the most important factors determining the tool wear rate. Tool wear rate is less affected by pulse off time and polarity. Using CNT and kerosene in a mixer creates a lubricating layer that protects both the tool and the work piece, resulting in a lower tool wear rate.

7.6 Effect of MWCNT-dielectric fluid on SR

At 17A, a pulse duration of 45 microseconds and a pulse duration of 60 microseconds, the mean SR for CNT + Kerosene

Table 6 Experimental data versus regression model comparison (Without CNT &With CNT MRR, TWR & SR)

RUN	Peak current	Pulse on time	Pulse off time	Without CNT MRR	With CNT MRR	Without CNT TWR	With CNT TWR	Without CNT SR	With CNT SR
1	17	45	30	17.363	20.5282	2.129	1.967	8.894	1.967
2	28	65	30	49.407	58.9771	6.962	6.451	15.593	6.451
3	28	65	60	37.885	45.0263	5.438	5.03	14.139	5.03
4	17	65	60	19.867	23.9258	3.591	3.294	11.373	3.294
5	21	55	30	27.996	34.0935	4.882	4.507	12.814	4.507
6	17	55	30	19.127	22.5067	2.871	2.647	11.147	2.647
7	21	55	60	20.649	24.4133	3.529	3.271	10.256	3.271
8	17	45	45	13.503	16.0645	1.045	0.956	9.57	0.956
9	21	45	45	18.197	21.6962	2.886	2.654	10.577	2.654
10	21	45	30	21.968	26.4802	2.931	2.723	11.078	2.723
11	28	55	45	38.611	46.8544	5.262	4.867	13.565	4.867
12	28	45	45	32.261	38.897	3.826	3.531	12.647	3.531
13	17	45	60	11.535	13.5397	1.258	1.165	7.346	1.165
14	21	65	45	25.566	30.1985	5.092	4.661	12.817	4.661
15	28	45	30	33.414	40.1502	4.189	3.907	12.673	3.907
16	21	65	30	29.789	35.3863	5.727	5.264	13.847	5.264
17	17	55	60	15.974	18.8221	2.124	1.953	11.418	1.953
18	17	65	45	22.254	26.2374	2.257	2.11	13.548	2.11
19	21	45	60	16.044	19.11	2.956	2.724	10.428	2.724
20	17	65	30	23.292	27.983	3.126	2.855	10.565	2.855
21	17	55	45	17.853	21.2325	2.056	1.898	11.82	1.898
22	28	45	60	24.63	29.1569	3.257	3.001	12.146	3.001
23	28	55	30	37.49	45.0554	6.148	5.645	14.625	5.645
24	28	65	45	43.038	52.0845	6.985	6.39	14.972	6.39
25	21	65	60	21.108	25.1016	4.881	4.489	11.776	4.489
26	28	55	60	27.636	32.9476	5.273	4.86	13.164	4.86
27	21	55	45	21.675	25.5418	4.779	4.396	12.455	4.396

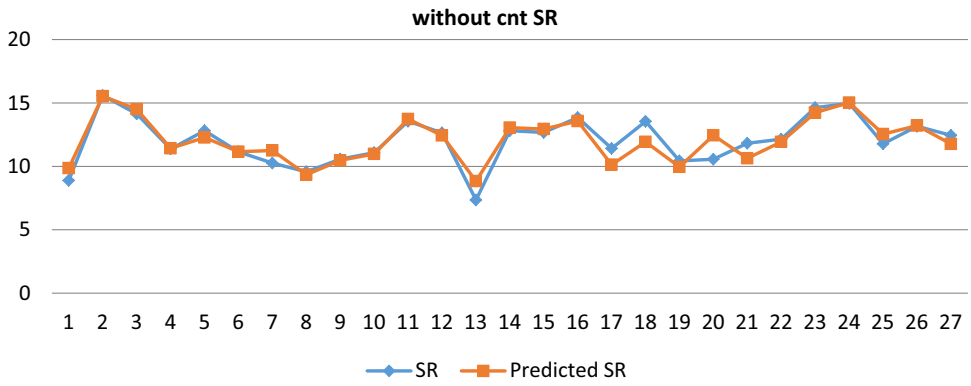

Fig. 11 Graph Illustration of the discrepancy between observed and expected SR in the absence of CNT

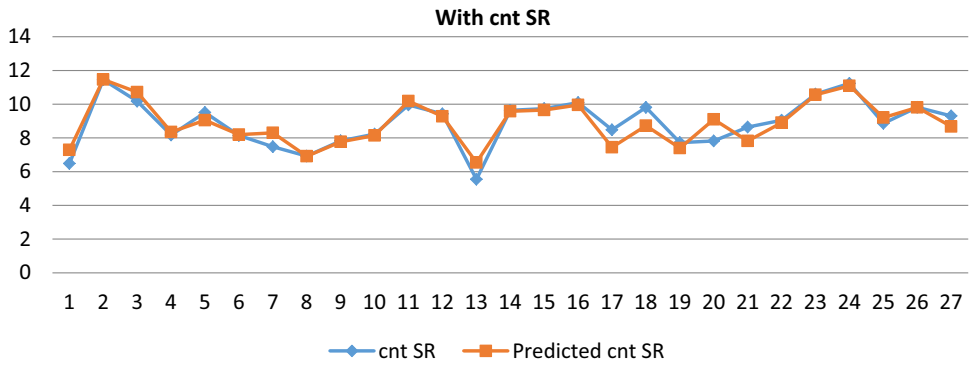

Fig. 12 Graph Illustration of the discrepancy between observed and expected SR in the presence of CNT

was 5.545 nm while the mean SR for pure Kerosene was 7.346 nm. Using CNT powder combined with dielectric helped smooth out the surface of the work piece.When more CNT powder was used, the surface roughness increased. An unstable arcing or short-circuiting caused the surface to deteriorate when the concentration in the gap was too high. It has a greasy feel and can be used as lubrication. The best surface roughness was attained using CNT.

8 Conclusion

In this experiment, three variables were considered: current, pulse on/ off time. The goal was to find the Surface Roughness, Material Removal Rate and Tool Wear Rate, as well as the effects of the variable parameters on these characteristics, both with CNT and without CNT. Aluminum was selected as the tool material, while EN -31 was selected as the work piece. For this set of studies, a full factorial design was developed. In the end, we came to the following conclusions. Each answer is affected differently by process parameters. The proportion contribution of significant parameters fluctuates as a function of the parameter's objective response.

(1) Peak current was shown to be the most important element in determining the MRR, followed by pulse on time, while pulse off time was determined to be the least important factor. The MRR rose in a straight line in direct proportion to the rise in current. The MRR increased linearly with longer pulse off times at first, then decreased marginally.
(2) It was found that the current was the most crucial factor in Surface Roughness, followed by the on time and then the off time. When the current was increased, the SR increased rapidly but not linearly. The objective was to increase the heart rate, hence SR was increased. Resonance decay (SR) rises with pulse off time. In a substantial way, surface roughness is affected by the length of time between pulses. When it comes to tool wear rate, peak current, pulse on time, and pulse off time are all critical.
(3) When using CNT and kerosene, the MRR was raised by an average of 19% with regard to the input parameter using carbon nano tubes, with the latter producing an MRR of 58.977 mm^3/min.
(4) Carbon nano tube reduced TWR by 8.51 percent on average when used with CNT and kerosene, and by 1.045 mm^3/min when used with pure kerosene, according to the results of the trial.
(5) The results of the tests showed that the surface roughness of the work piece was reduced from 7.346 micro meters for pure kerosene to 5.545 micro meters when MWCNT powder was mixed with dielectric. When MWCNT were used together as a dielectric fluid, the quality of the surface was enhanced by an average of 30 percent.

9 Future scope

The following suggestions may prove useful for future work:

- The present work was only concern with the experimental investigation of three process parameters like peak current, pulse on time and pulse off time on MRR, SR and TWR, so It will be important to study the influence of other EDM process parameters like gap voltage, polarity, and spark gap distance on different output like MRR, SR and TWR.
- Investigation EDM parameter with different powder mixed in dielectric fluid like carbon, silicon, Aluminum, etc.with different electrode as copper, brass, carbon.

Declarations

Conflict of interest No potential conflict of interest was reported by the author(s).

References

1. Gautam Kocher, K, Chopra. G., Chopra K, Kumar E, Riet PE (2012) Investigation of surface integKocher. In: Investigation of Surface Integrity of AISI D3 Tool Steel After EDM
2. Darji, Y.A. Multi-parameter analysis and modeling of MRR & SR on electro discharge machine with multi wall carbon nano tube
3. Ghoreishi, M., Tabari, C.: Investigation into the effect of voltage excitation of pre-ignition spark pulse on the electro-discharge machining (EDM) process. Mater Manuf. Process **22**, 833–841 (2007). https://doi.org/10.1080/10426910701446812
4. Darji, Y., Koradiya, P.L., Shah, J.R.: Experiment investigation of EDM parameter MRR and TWR with multi wall carbon nano tubes. Int. J. Mech. Eng. Technol. (IJMET) **5**(7), 84–192 (2014)
5. Salman, Ö., Kayacan, M.C.: Evolutionary programming method for modeling the EDM parameters for roughness. J. Mater. Process. Technol. **200**(1–3), 347–355 (2008)
6. Dastagiri, M., Kumar, A.H.: Experimental investigation of EDM parameters on stainless steel&En41b. Procedia Eng. **1**(97), 1551–1564 (2014)
7. Marichamy, S., Saravanan, M., Ravichandran, M., Stalin, B.: Optimization of surface roughness for duplex brass alloy in EDM using response surface methodology. Mech. Mech. Eng. **21**(1), 57–66 (2017)
8. Syed, K.H., Palaniyandi, K.: Performance of electrical discharge machining using aluminium powder suspended distilled water. Turk. J. Eng. Environ. Sci. **36**(3), 195–207 (2012)
9. Hyun-Seok, T.A., Chang-Seung, H.A., Ho-Jun, L.E., Hyung-Woo, L.E., Jeong, Y.K., Myung-Chang, K.A.: Characteristic evaluation of Al2O3/CNTs hybrid materials for micro-electrical discharge machining. Trans. Nonferrous Met. Soc. China **1**(21), s28-32 (2011)
10. Khan, A.A.: Electrode wear and material removal rate during EDM of aluminum and mild steel using copper and brass electrodes. Int. J. Adv. Manuf. Technol. **39**, 482–487 (2008)
11. Kiyak, M., Çakır, O.: Examination of machining parameters on surface roughness in EDM of tool steel. J. Mater. Process. Technol. **191**(1–3), 141–144 (2007)
12. Rizvi, S.A., Agarwal, S. An investigation on surface integrity in EDM process with a copper tungsten electrode. Procedia Cirp. **42**, 612–627 (2016)
13. Torres, A., Luis, C.J., Puertas, I. Analysis of the influence of EDM parameters on surface finish, material removal rate, and electrode wear of an INCONEL 600 alloy. Int. J. Adv. Manuf. Technol. **80**(1–4), 123–140 (2015)
14. Janmanee, P., Muttamara, A.: Performance of difference electrode materials in electrical discharge machining of tungsten carbide. Energy Res. J. **1**(2), 87–90 (2010)
15. Suryakant, T., Allurkar, B. Literature review on electric discharge machining. Int. J. Sci. Eng. Technol. Res. **5**(2), 404–406 (2016)
16. Arrazola, P.J., Özel, T., Umbrello, D., Davies, M., Jawahir, I.S. Recent advances in modelling of metal machining processes. CIRP. Ann. **62**(2), 695–718 (2013)
17. Mitsui, K., Mahardika, M.: A new method for monitoring micro-electric discharge machining process. Int. J. Machine Tools Manuf. **48**, 446–458 (2008)
18. Puertas, I., Luis, C.J.: A study of optimization of machining parameters for electrical discharge machining of boron carbide. Mater. Manuf. Processes **19**(6), 1041–1070 (2004)
19. Liu, K., Lauwers, B., Reynaerts, D.: Process capabilities of Micro-EDM and its applications. Int. J. Adv. Manuf. Technol. **47**, 11–19 (2010)
20. Mai, C., Hocheng, H., Huang, S.: Advantages of carbon nanotubes in electrical discharge machining. Int. J. Adv. Manuf. Technol. **59**, 111–117 (2012)
21. Chamsa-Ard, W., Brundavanam, S., Fung, C.C., Fawcett, D., Poinern, G.: Nanofluid types, their synthesis, properties and incorporation in direct solar thermal collectors: A review. Nanomaterials **7**(6), 131 (2017)
22. Hameed, A., Mukhtar, A., Shafiq, U., Qizilbash, M., Khan, M.S., Rashid, T., Bavoh, C.B., Rehman, W.U., Guardo, A.: Experimental investigation on synthesis, characterization, stability, thermophysical properties and rheological behavior of MWCNTs-kapok seed oil based nanofluid. J. Mol. Liq. **1**(277), 812–824 (2019)
23. Tomadi, S. H., Hassan, M. A., Hamedon, Z., Daud, R., Khalid, A.G. Analysis of the influence of EDM parameters on surface quality, material removal rate and electrode wear of tungsten carbide. In: Proceedings of the International Multi Conference of Engineers and Computer Scientists 2009 (Vol. 2, pp. 18–20)
24. Tsai, H.C., Yan, B.H., Huang, F.Y.: EDM performance of Cr/Cu-based composite electrodes. Int. J. Mach. Tools Manuf **43**(3), 245–252 (2003)
25. Li, L., Wong, Y.S., Fuh, J.Y., Lu, L.: EDM performance of TiC/copper-based sintered electrodes. Mater. Des. **22**(8), 669–678 (2001)